Available online at www.sciencedirect.com

SciVerse ScienceDirect

Advances in Space Research 50 (2012) 211–220

ADVANCES IN SPACE RESEARCH (a COSPAR publication)

www.elsevier.com/locate/asr

A nonlinear background removal method for seismo-ionospheric anomaly analysis under a complex solar activity scenario: A case study of the M9.0 Tohoku earthquake

Liming He [a], Lixin Wu [a,b,*], Sergey Pulinets [c], Shanjun Liu [a], Fan Yang [a]

[a] Institute for Geo-informatics & Digital Mine Research, College of Resources and Civil Engineering, Northeastern University, Shenyang 110819, PR China
[b] Academy of Disaster Reduction and Emergency Management, Beijing Normal University, Beijing 100875, PR China
[c] Fiodorov Institute of Applied Geophysics, Roshydromet, Moscow 129128, Russia

Received 22 November 2011; received in revised form 29 March 2012; accepted 1 April 2012
Available online 10 April 2012

Abstract

A precise determination of ionospheric total electron content (TEC) anomaly variations that are likely associated with large earthquakes as observed by global positioning system (GPS) requires the elimination of the ionospheric effect from irregular solar electromagnetic radiation. In particular, revealing the seismo-ionospheric anomalies when earthquakes occurred during periods of high solar activity is of utmost importance. To overcome this constraint, a multiresolution time series processing technique based on wavelet transform applicable to global ionosphere map (GIM) TEC data was used to remove the nonlinear effect from solar radiation for the earthquake that struck Tohoku, Japan, on 11 March, 2011. As a result, it was found that the extracted TEC have a good correlation with the measured solar extreme ultraviolet flux in 26–34 nm (EUV_{26-34}) and the 10.7 cm solar radio flux ($F_{10.7}$). After removing the influence of solar radiation origin in GIM TEC, the analysis results show that the TEC around the forthcoming epicenter and its conjugate were significantly enhanced in the afternoon period of 8 March 2011, 3 days before the earthquake. The spatial distributions of the TEC anomalous and extreme enhancements indicate that the earthquake preparation process had brought with a TEC anomaly area of size approximately 1650 and 5700 km in the latitudinal and longitudinal directions, respectively.

Keywords: Total electron content (TEC); Solar electromagnetic radiation; Multiresolution wavelet transform (MWT); Earthquake; Anomaly recognition

1. Introduction

Over the past two decades, there have been extensive studies on seismo-ionospheric anomalies that precede earthquakes (Chen et al., 1999; Liu et al., 2000; Pulinets and Boyarchuk, 2004; Rishbeth, 2006; Zhao et al., 2008; Klimenko et al., 2011; Kon et al., 2011; Xu et al., 2011). Statistical studies show that ionospheric disturbances caused by seismic activities can be observed between several days and a few minutes prior to an impending large earthquake ($M \geqslant 6$) (Liu et al., 2000, 2004a, 2006; Le et al., 2011). However, in many cases, ionospheric anomaly signals induced by seismic activity can easily be confused with background fluctuations due to solar activity. Afraimovich et al. (2008) showed that TEC anomalies observed within the area of a coming earthquake could be caused not as much by the enhanced seismic activity before earthquakes as by the changes in the global ionization due to the dynamics of the solar radiation. Debates and doubts still exist about pre-earthquake ionospheric anomalies (Rishbeth, 2006, 2007; Dautermann et al., 2007; Afraimovich and Astafyeva, 2008). Therefore, removing ionospheric variations resulting from irregular solar electromagnetic

* Corresponding author at: Institute for Geo-informatics & Digital Mine Research, College of Resources and Civil Engineering, Northeastern University, Shenyang 110819, PR China. Tel./fax: +86 10 58806340.
E-mail addresses: heliming@mail.neu.edu.cn (L. He), awulixin@263.net (L. Wu), pulse1549@gmail.com (S. Pulinets), liusjdr@126.com (S. Liu), yangfan1101664@126.com (F. Yang).

0273-1177/$36.00 © 2012 Published by Elsevier Ltd. on behalf of COSPAR.
http://dx.doi.org/10.1016/j.asr.2012.04.001

radiation before seismo-ionospheric data analysis turns to be of utmost importance.

The ionosphere is a product of the interaction between the Sun and the Earth's environment. The Earth's upper atmosphere absorbs solar radiation, which results in ionosphere heating, dissociation and ionization. Therefore, the total electron content (TEC) of the ionosphere is mainly controlled by the intensities of solar electromagnetic radiation. In periods of increasing solar activity, solar radiation variations over the short timescale (e.g., months, seasons) are intensive, rapid and nonlinear. For ionospheric data analysis, the solar radiation background in a signal is just like noise, which often increases difficulties in further processing, as the background always blurs the analytical signal. It is difficult or even impossible to analyze a signal with a strong background. Examples of earthquakes are always chosen for analysis under quiet geophysical and space weather conditions, such as the Wenchuan earthquake, which occurred in the period of extremely low solar activity between the 23rd and the 24th solar cycle. However, earthquakes can happened at any time around the world. Therefore, knowing how to detect and reveal the ionospheric anomaly variations, such as the M9.0 Tohoku earthquake, which occurred during a period of high solar activity, is a difficult problem yet to be adequately resolved.

Solar extreme ultraviolet (EUV) irradiances are the fundamental and primary energy input for the Earth's ionosphere and thermosphere (Tobiska, 1996). At present, several space-flight instruments can provide EUV data including the Solar EUV Monitor (SEM) (Judge et al., 1998) on the Solar and Heliospheric Observatory (SOHO), the Solar EUV Experiment (SEE) (Woods et al., 2005) on the Thermosphere–Ionosphere–Mesosphere Energetics and Dynamics (TIMED) satellite and the Extreme ultraviolet Variability Experiment (EVE) (Woods et al., 2010) on the NASA Solar Dynamics Observatory (SDO) mission. Since 1996, the solar EUV fluxes in 26–34 nm ($EUV_{26–34}$) with a time resolution of 15 s was continuously monitored by the highly accurate and stable EUV spectrometer (SEM) aboard SOHO satellite. Therefore, we utilized the $EUV_{26–34}$ data from January 2011 to March 2011 provided by the Space Sciences Center of University of Southern California (http://www.usc.edu/dept/space_science/semdatafolder/long/15_sec_avg/) in this paper. Moreover, there are many commonly-used solar proxies including $F_{10.7}$ (10.7 cm solar radio flux), SSN (sunspot number) and Mg II core-to-wing ratio (Viereck et al., 2001), etc. The $F_{10.7}$ is a measure of the solar radio flux per unit frequency at a wavelength of 10.7 cm, near the peak of the observed solar radio emission. The index has a good relationship with the solar cycle. Therefore, when describing solar activity, it was widely used as a representative index. In this paper, we also use the daily data of $F_{10.7}$ from January 2011 to March 2011 provided by the National Oceanic and Atmospheric Administration (NOAA) Data Center (ftp://ftp.ngdc.noaa.gov). Fig. 1 shows that the $EUV_{26–34}$ increased 1.45-fold (from 1.1 to 1.6) (in units of 10^{14} photons/m^2/s), and the $F_{10.7}$ increased more than 2-fold (from 77 to 164) (in units of 10^{-22} W/m^2/Hz) during the observation period. It is noteworthy that the $EUV_{26–34}$ and the $F_{10.7}$ have a very similar variation tendency. What is more important, both the two indices indicated that the variations in environmental background from solar fluxes were rapid and had a nonlinear character before the shocking. Therefore, an important challenge in processing the data is to develop an effective method to remove the strong and nonlinear background and to extract reliable physical information.

Wavelet transform is a modern nonlinear data processing method and has been one of the most effective tools to analyze the nonstationary signals (Mallat, 2008). By the wavelet transform, in the low frequency part of the signal, a lower time resolution and a higher frequency resolution are used, whereas in the high frequency part, a higher time resolution and a lower frequency resolution are utilized, allowing any details of the signal to be focused on. By means of the multiresolution wavelet transform (MWT), an original signal can be decomposed into localized contributions characterized by a scale parameter. Each contribution represents a portion of the signal with a different frequency. In the present paper, MWT was used to eliminate the background from solar radiation in ionospheric TEC data. As shown in Fig. 1, the solar radiation signal is a low frequency over the short timescale (e.g., months, seasons). Hence, a pure analyte signal can be created through wavelet reconstruction by the wavelet decomposition of the TEC dataset and by removal of the background contribution in the wavelet transformed vector. The presented algorithm consists of two parts: low-frequency (approximation) removal based on a wavelet decomposition algorithm, and an evaluation of the results.

2. Ionosphere data

With the unprecedented temporal and spatial coverage of the observations based on the global positioning system (GPS) satellites and the corresponding hundreds of ground stations distributed all over the world, the ionospheric TEC data have been extensively utilized in ionospheric studies to detect and measure ionospheric anomaly variations. The ionospheric data used in this study were generated on a daily basis at Center for Orbit Determination in Europe (CODE) using TEC data from approximately 250 continuously operating GPS receivers of the International GNSS Service (IGS) and other institutions. CODE TEC maps were generated every 2 h to produce 2 hourly snapshots of the global ionosphere. Each global ionosphere map (GIM) has a spatial resolution of $2.5° \times 5°$ in geographic latitude and longitude. According to Dobrovolsky et al. (1979), the Tohoku earthquake likely caused large-scale ionospheric disturbances because it has very high intensity ($M = 9.0$). Therefore it is highly possible to find some large-scale structures and variations in the ionosphere from the CODE TEC data.

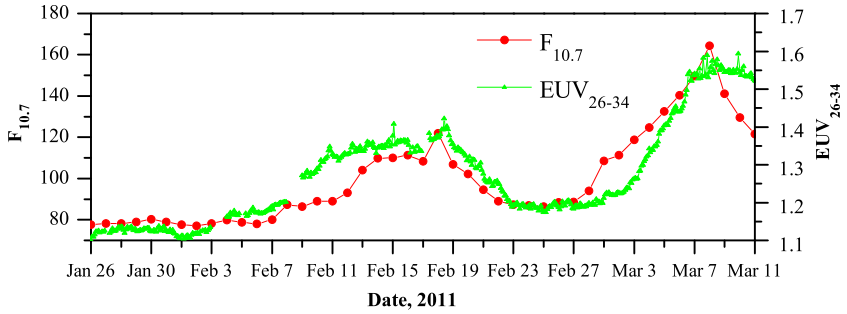

Fig. 1. The solar activity time series, from 26 January to 11 March, 2011, of 2 h average SOHO/SEM 26–34 nm EUV flux (in units of 10^{14} photons/m^2/s), and the $F_{10.7}$ index (in units of 10^{-22} W/m^2/Hz).

We utilized CODE GIMs (ftp://cddisa.gsfc.nasa.gov/pub/gps/products/ionex) for the period from 10 February to 11 March 2011 in this paper.

3. Methodology

In this section we discuss in detail the MWT-based data processing technique applied to reveal the short temporal scale nonlinear variations of solar radiation in GIMs. In the first subsection we address the key theories that constitute the building blocks of the presented technique. Next, the quantification index of the method is described.

3.1. Theory and calculation

A wavelet is defined as a series of functions $\psi_{u,s}(t)$ derived from a function $\psi(t)$ by shifts in the translations and dilations that act on the frequency variable as follows

$$\psi_{u,s}(t) = \frac{1}{\sqrt{s}}\psi\left(\frac{t-u}{s}\right), \quad s \neq 0, \quad u, s \in R, \tag{1}$$

where ψ is a so-called mother wavelet, and s and u denote the dilation and translation parameters, respectively. If $f(t)$ is an energy-limited signal, then the continuous wavelet transform can be expressed as

$$W(u,s) = \frac{1}{\sqrt{s}}\int_{-\infty}^{+\infty} f(t)\psi^*\left(\frac{t-u}{s}\right)dt, \tag{2}$$

In practice, the signals to be analyzed are generally discrete. Therefore, the discrete forms for a continuous wavelet and its transform are generally needed. Despite the existence of several algorithms (Grossman and Morlet, 1984; Hilton, 1997), the multiresolution signal decomposition and reconstruction by Mallat (1989a,b) is commonly used. If $A_0(n), n \in Z$ denotes a discrete signal of ionospheric TEC, the decomposition can be calculated by

$$A_j(n) = \sum_{k\in Z} h_k A_{j-1}(n - 2^{j-1}k), \tag{3}$$

$$D_j(n) = \sum_{k\in Z} g_k D_{j-1}(n - 2^{j-1}k), \tag{4}$$

and the reconstruction of the original signal A_0 uses a discrete dyadic wavelet transform. The calculation can then be performed by

$$A_{j-1}(n) = \sum_{k\in Z} \tilde{h}_k A_j(n - 2^{j-1}k) + \sum_{k\in Z} \tilde{g}_k D_j(n - 2^{j-1}k), \tag{5}$$

where $j\ (= 1 \ldots J)$ are the times of decomposition, $\{h_k\}_{k\epsilon Z}$, $\{g_k\}_{k\epsilon Z}$ and $\{\tilde{h}_k\}_{k\in Z}, \{\tilde{g}_k\}_{k\in Z}$ are discrete filters and conjugate filters obtained from the basic function $\psi(t)$ and the corresponding scaling function $\psi_{u,s}(t)$, respectively (Mallat, 1989b). A_j and D_j are called the discrete approximation and the discrete detail at the jth level or at the resolution of 2^j with respect to A_0, respectively. A_j is the low frequency part of signal A_0 with a frequency lower than 2^{-j}, and D_j is the high frequency part of the signal with the frequency between 2^{-j} and 2^{-j+1} (Shao et al., 1998).

For the decomposition of each GIM pixel, the A_j and D_j values are the different frequency components of the original ionospheric signal. The GIM TEC oscillation will be decomposed into the D_j and the background effect of solar radiation will remain in A_j if the j is properly selected. Therefore, the extraction of the TEC variations of solar radiation from the GIM TEC can be easily implemented by reconstructing the signal from A_j and D_j with the A_j values being set to zero.

3.2. Quantification

To evaluate the obtained coefficients of the GIM TEC after preprocessing with MWT, the correlations between the obtained background and the measured solar activity indices EUV_{26-34} and $F_{10.7}$ are calculated, respectively. The EUV_{26-34} measurements have a high time resolution of 15 s, but the GIM TEC data only have a time resolution of 2 h. Therefore, the 2 h average EUV_{26-34} calculated for each day in each pixel are used. However, the $F_{10.7}$ data utilized are of poorer time resolution (1 day) than the GIM TEC data utilized. Therefore, the 1 day mean GIM TEC decomposed coefficients calculated for each day in each pixel are used. For the set of N measurements of the quantity X in the solar activity indices and the quantity Y in the GIM TEC data, the Pearson product–moment correlation coefficient is calculated by

$$R(X,Y) = \frac{\sum_{i=1}^{N}(X_i - \bar{X})(Y_i - Y)}{\sqrt{\sum_{i=1}^{N}(X_i - \bar{X})^2}\sqrt{\sum_{i=1}^{N}(Y_i - \bar{Y})^2}}, \tag{6}$$

where an overbar on a quantity in Eq. (6) denotes the mean of the N values. The linear correlation coefficient is a measure of how strongly a variation in X results in a variation of Y. A perfect correlation is $R = 1$, a complete anticorrelation is $R = -1$, and uncorrelated data yield is $R \sim 0$. If there are N data points, the uncorrelation is consistent with $|R| \leqslant 2/\sqrt{N}$, while $|R| > 2/\sqrt{N}$ represents a correlation at the 95% confidence level (Borovsky et al., 1998; Bendat and Piersol, 2010).

4. Results

4.1. Selection of the wavelet base

There are many different wavelet families up to the present. An important aspect of selecting wavelet is to choose a wavelet with more vanishing moments than the polynomial order of the signal being analyzed. The physical meaning of vanishing moments can be considered as a convergence rate by which the wavelet function approximates a signal. Therefore, the vanishing moments of a wavelet have a significant impact on signal feature extraction. Another important aspect of the choice of a wavelet is the support length. The narrower the compactly supported width or the faster the decay is, the better the localization property of the wavelet. In this paper, the Daubechies wavelets were tested for the ability to eliminate background. It should be stressed that there are an enormous number of possible wavelet bases. The Daubechies wavelets are smooth, orthogonal, and compactly supported (Daubechies, 1992). For the dbN wavelet, the number of vanishing moments of ψ is N, and the support length of ψ is $2N - 1$. The greater the order N of the wavelet function is, the stronger the ability to reflect the details of the high frequency of the signal. In background removal, we are more concerned about the low frequency components of ionospheric TEC signal, thus it is not required that N is especially high. In addition, the compact support in fixed intervals and a sufficient order of vanishing moments should be met to analyze the TEC signal effectively when selecting the wavelet base to remove the background. Therefore, the popular db3 wavelet is a good choice for low-frequency signal extraction such as the TEC variation signal from solar radiation. Through the above analysis, the db3 wavelet has been chosen as the wavelet base in this work.

4.2. Influence of the decomposition number

Once the wavelet function for background removal is decided, the optimal decomposition level should be determined to obtain the best background removal effect. With the increase in decomposition number, the analyte signal contribution was gradually excluded from the ionospheric TEC. If the number was too small, the background would involve too much information from the analyte signal. This is to say that the background would be over-subtracted, and the concentration of the analyte signal would be underestimated. In contrast, too much decomposition would result in an excessively low estimation of the background and a large error. The proper decomposition number could be determined by a visual inspection of the processed TEC signal. In this study, the appropriate decomposition number was found to be 6 according to the practical behavior of the solar radiation background in ionospheric TEC.

4.3. Elimination of nonlinear backgrounds

The above-mentioned approach was applied to the GIM TEC dataset. Fig. 2(a) shows the original GIM TEC of the epicenter pixel from 26 January to 11 March, 2011. It can be seen that the TEC data are affected by the background. From Fig. 2(b)–(h), it can be observed that the original TEC is decomposed into high frequency contributions (details D_j ($j = 1, \ldots, 6$)) and low frequency contributions (approximation A_6). It is clear that the information from the ionospheric TEC oscillation is decomposed into the D_j's, and that A_6 represents the solar background variations. Therefore, if we reconstruct the TEC from the D_j's components only, we will obtain the TEC without the background effect. Fig. 2(i) shows the reconstructed signal of the TEC. The background is subsequently subtracted from the original TEC, and the net analyte signal is thus created.

In order to gain further insight into the ionospheric perturbations around the globe, an analysis of all the pixels in the GIMs was conducted. Each GIM covers ±87.5 latitude and ±180 longitude, with spatial resolutions of 2.5° and 5°, respectively. Therefore, each map consists of 5112 (=71 × 72) grid points. For each pixel of the GIMs within the examined period, we repeat the above process, and then the net GIMs without the effect from solar radiation are obtained.

4.4. Evaluation of the results

4.4.1. Correlation of the epicenter pixel

The proposed approach was also evaluated by the solar activity measurement indices EUV_{26-34} and $F_{10.7}$. Here, we take the epicenter pixel of GIMs as an example to illustrate feasibility. Fig. 3 shows the time series of solar indices EUV_{26-34} and $F_{10.7}$, the decomposed TEC approximation (TEC_{A6}) and the correlations between the TEC_{A6} and the two solar indices. Comparing Fig. 3(a) with (b), it is evident that the variations of the wavelet's 6th-order approximation are similar to the EUV_{26-34} and $F_{10.7}$. In contrast to the variation of the EUV_{26-34} and $F_{10.7}$, the decomposed TEC_{A6} increased more than 2.6-fold (from 7.1 TECU to 18.5 TECU) during the same observation period. We can also note that, on the increasing phase, TEC_{A6} and the two solar indices are very close. The recovery phase shows the difference, about 2–3 days of ionosphere reaction delay in comparison with EUV_{26-34} and $F_{10.7}$, which is corresponding to the conclusions of Afraimovich et al. (2008).

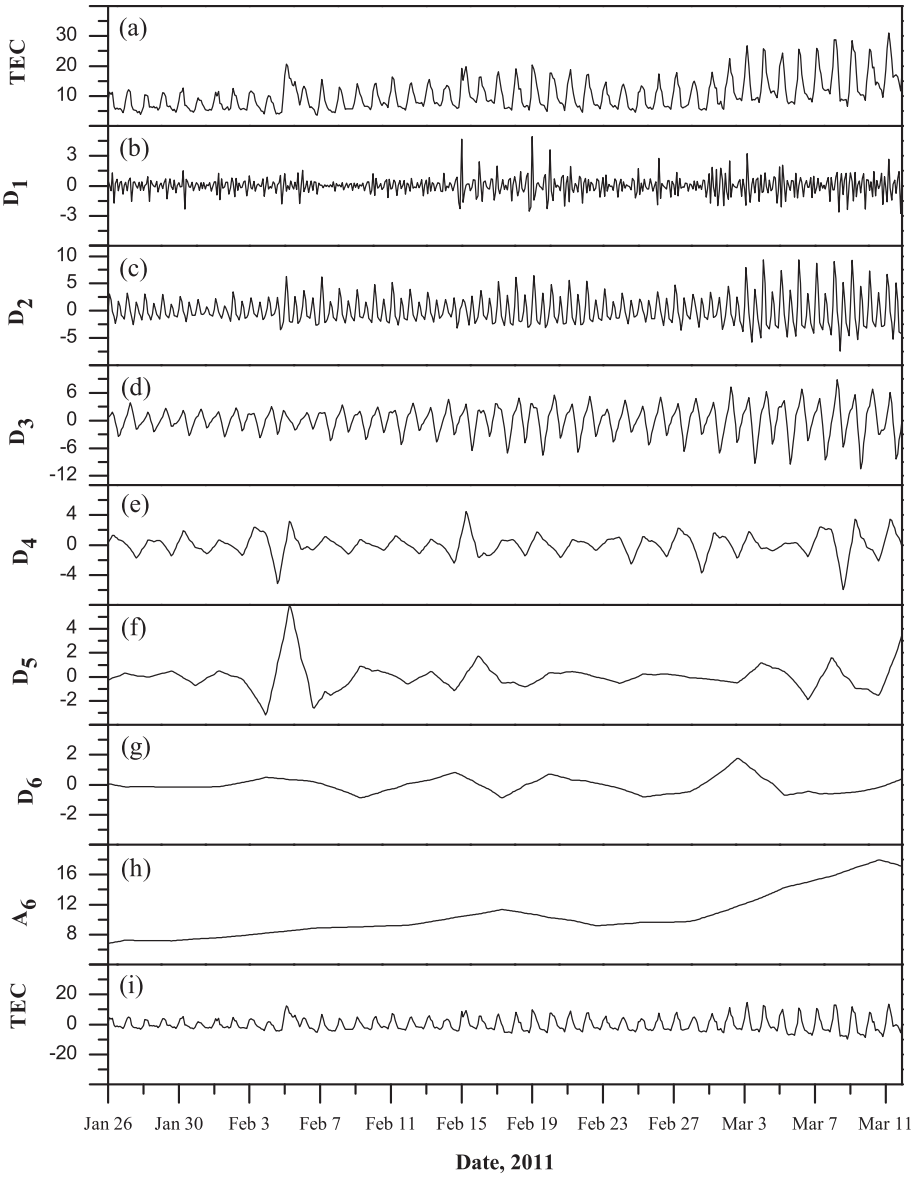

Fig. 2. (a) The original TEC over the epicenter of the Tohoku earthquake. (b–h) Details (D_1–D_6) and approximation (A6) of the original TEC from a six-level multiresolution wavelet transform using the db3 wavelet. (i) The reconstructed TEC signal after removing the background.

We further demonstrate the Pearson correlation analysis as mentioned above to evaluate the relations between TEC_{A6} and the two solar indices. It can be seen that the trends of the two solar indices and TEC_{A6} are very similar, which means that the relationship between the variables is a highly linear correlation. As shown in Fig. 3c, the linear correlation coefficient between TEC_{A6} and $F_{10.7}$ reach 0.9157, and the linear correlation coefficient between TEC_{A6} and $EUV_{26–34}$ is the similar up to 0.9061. Therefore, the nonlinear influence from solar radiation at the monthly timescale can be efficiently removed through the MWT-based method by eliminating the wavelet's 6th-order approximation.

4.4.2. Correlation of global pixels

To check if the correlations between the two solar indices ($EUV_{26–34}$ and $F_{10.7}$) and TEC_{A6} are significant all over the globe, a spatial analysis is conducted. Fig. 4 presents the global correlation coefficient map during the examined time period. It can be seen that the extracted solar background has remarkable positive correlations with both the two solar flux indices in most regions around the globe. Therefore, the method presented in this paper can be used to remove the background in the ionospheric TEC induced by solar radiation variations. It is noteworthy that there are slight negative correlations between the extracted background and the two solar flux indices in the Antarctic region.

5. Comparison with the traditional method

A considerable amount of research has been devoted to the study of the ionospheric anomaly variabilities due to seismic activities. Such studies are of great importance for the link between the ionosphere anomalies and

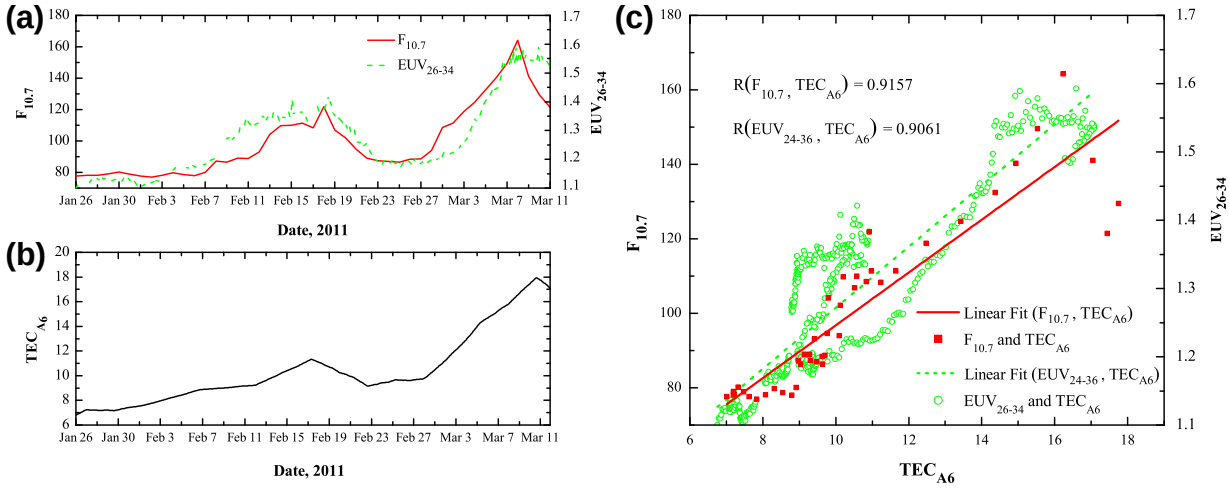

Fig. 3. (a) Solar activity time series of $EUV_{26–34}$ and $F_{10.7}$. (b) Decomposed TEC variation TEC_{A6} time series of epicenter pixel of the Tohoku earthquake. (c) Comparison of the TEC_{A6} and $F_{10.7}$ (in red color), and the TEC_{A6} and $EUV_{26–34}$ (in green color). (For interpretation of the references to colour in this figure legend, the reader is referred to the web version of this article.)

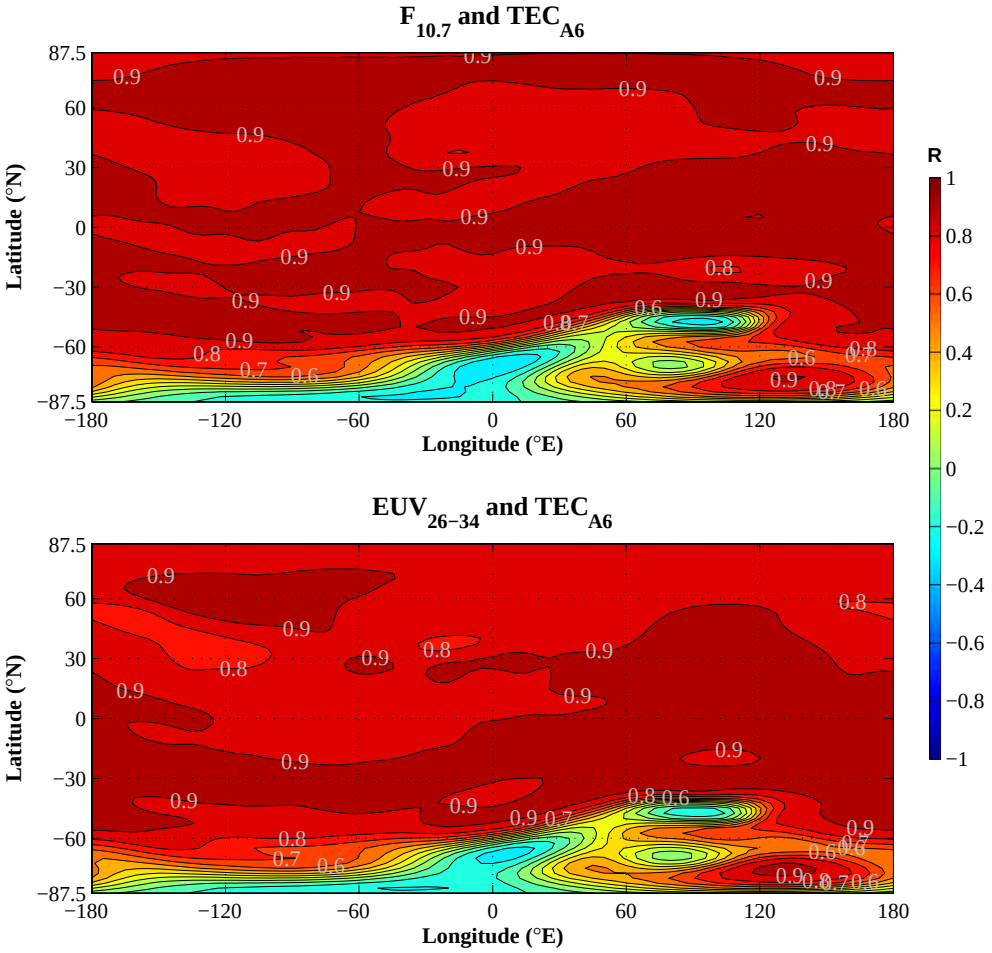

Fig. 4. The global correlation coefficients between the extracted solar background (TEC_{A6}) and the measured solar activity indices during the examined time period. Top: $F_{10.7}$ and TEC_{A6}; Bottom: $EUV_{26–34}$ and TEC_{A6}. (For interpretation to colours in this figure, the reader is referred to the web version of this paper.).

earthquakes. However, little attention has been devoted to removing the effect from solar radiation variation. These studies may have been more reasonable if this situation had been considered. With the Tohoku earthquake being an example, this paper aims to illustrate the importance of the presented method. Current method developed by

Liu et al. (2009, 2011) has been widely utilized in seismo-ionospheric anomaly analysis. Fig. 5 displays grid points with extremely enhanced differences obtained by the traditional method occurring from 0000 UT to 2200 UT on 8 March 2011, which indicates that the solar radiation background blurs the analytical TEC signals. The ionosphere was disturbed at a global scale during the period 0000–2200 UT on 8 March 2011. Fig. 6 demonstrates the improved results obtained by the new method at the same time period on 8 March 2011. It can be observed that the strong background in the global scale can be removed quite well after the preprocessing by the MWT-based method. In fact, the GIM TEC under study was enhanced significantly in an area of approximately 15° in latitude and 60° in longitude around the epicenter during the afternoon periods of day 3 (8 March 2011) before the Tohoku earthquake. Because 1° corresponds to about 110 km in latitude and 95 km in longitude, the TEC anomalous size of the Tohoku earthquake is approximately 1650 and 5700 km in the latitudinal and the longitudinal directions, respectively.

6. Discussion and conclusion

In the condition of strong solar activity, we proposed a novel method for ionospheric TEC data preprocessing to reveal the ionospheric anomalies probably associated with the Tohoku earthquake. It is found that there were pronounced enhancements appeared on 8 March 2011, 3 days before the shocking. The main properties of the TEC anomaly variations that occurred on 8 March 2011 are displayed in the Fig. 6, and can be summarized as follows,

(1) The ionospheric perturbations have localization features. The grids of extreme maximum increments of TEC appeared mainly around the epicenter and the conjugate region during the whole observation period, and there was no other obvious increment on global scale.
(2) The position of the first occurrence, the position of extinction, and the dynamic development process of ionospheric perturbations have nice spatial correlations around the epicenter throughout.
(3) The appearance time of the peak value of ionospheric perturbations has regularity, centered at approximately 0400–1000 UT (1300–1900 LT).

All these characteristics generally agree with the previous studies in Asia (Liu et al., 2000, 2004b, 2006, 2009; Chen et al., 2004; Zhao et al., 2008; Kon et al., 2011). In addition,

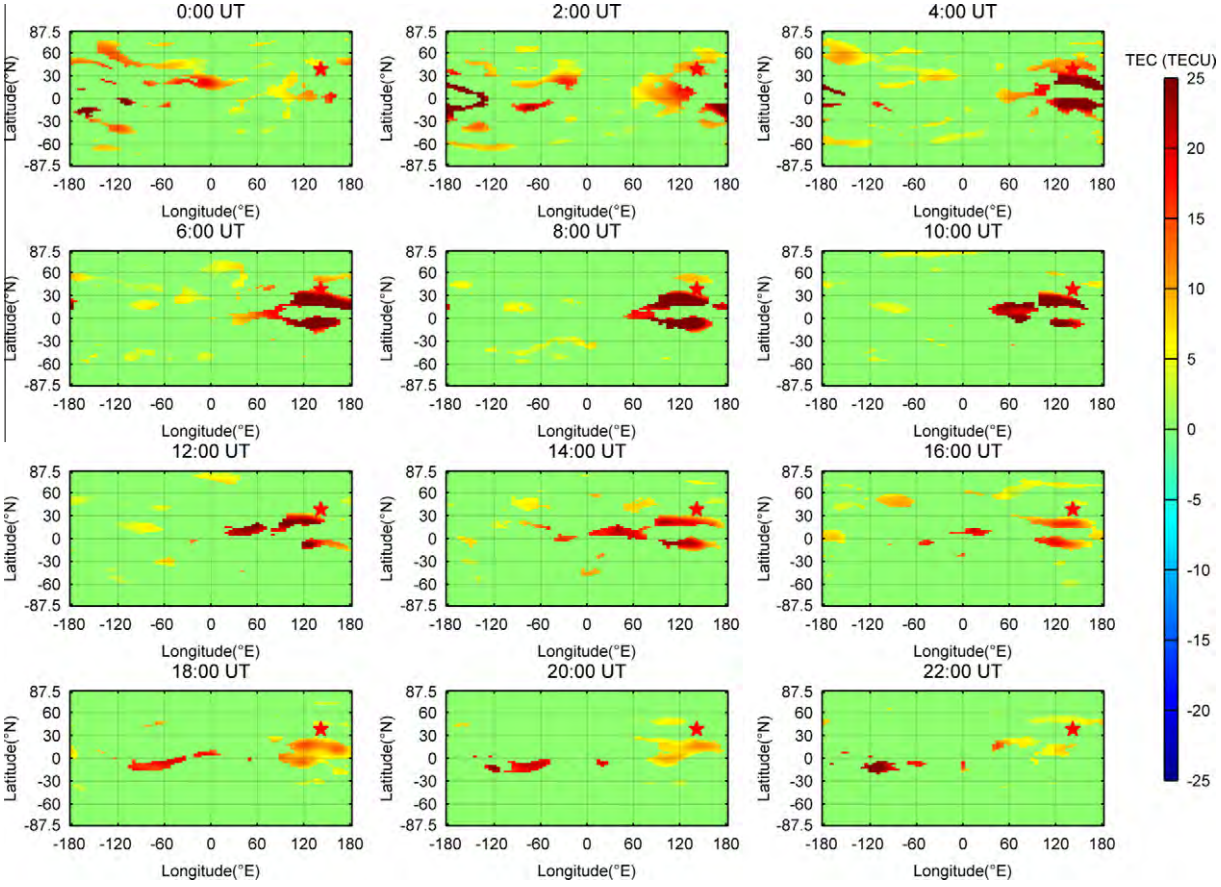

Fig. 5. The extreme enhancements extracted by the traditional method in each grid point of the 30-day period that appeared from 0000 UT to 2200 UT on 8 March 2011. The color denotes the difference of the TEC observed on 8 March 2011 from the 1–15 previous days' moving median. The red star shows the epicenter (38.32°N, 142.37°E) of the Tohoku earthquake.

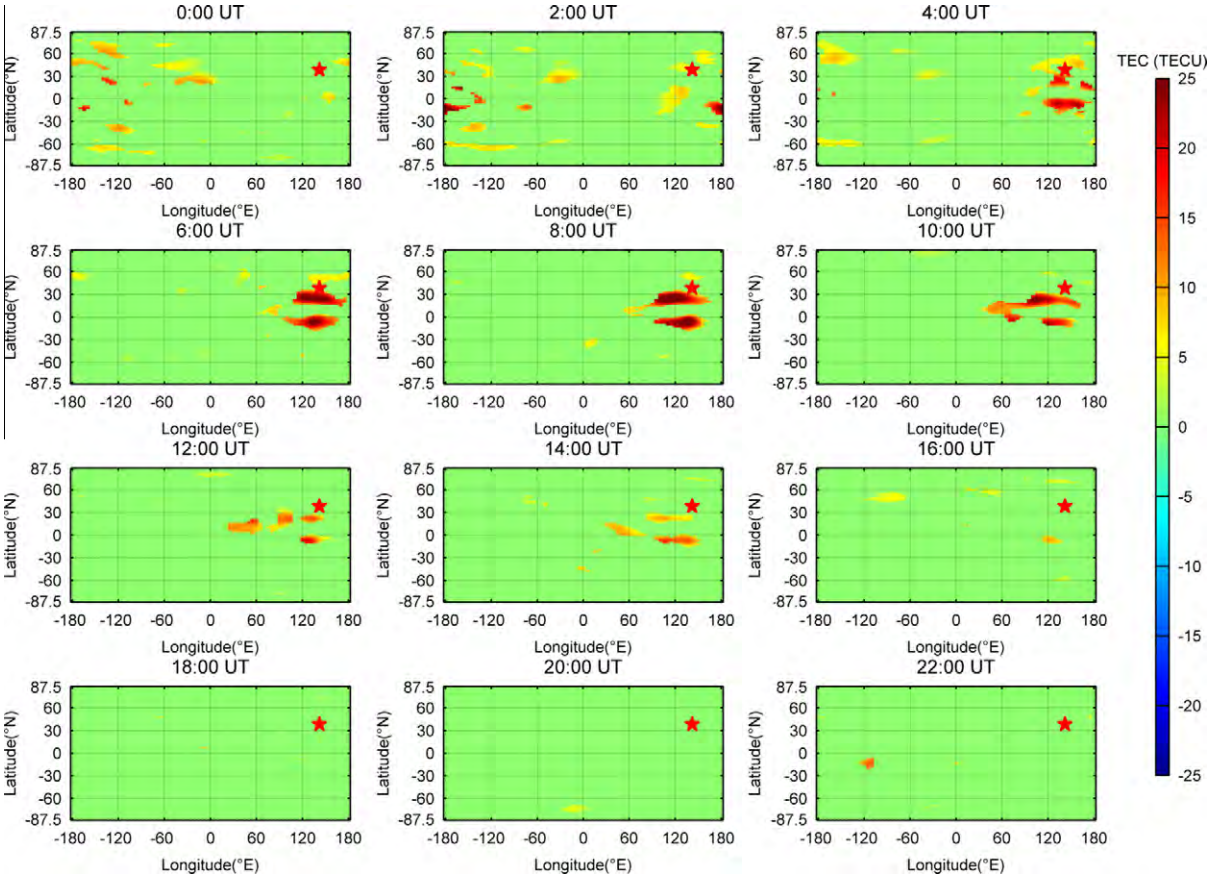

Fig. 6. As Fig. 5, but for the extreme enhancements extracted by the method presented in this paper. (For interpretation of the references to colour in this figure legend, the reader is referred to the web version of this article.)

similar enhanced anomalies in the afternoon period of 8 March 2011 (3 days before the earthquake) in the GIM TEC are also observed by Xu et al. (2011). They pointed out that the giant positive disturbance was possibly associated with the impending disastrous earthquake and contributed from the enhanced solar radiation. It means that the ionospheric TEC anomalies appeared on March 8, 2011 induced by seismic activity are confused with rapid fluctuations due to solar activity. However, they only analyzed the anomaly by qualitative analysis, and did not gain further insights into the quantitative analysis of the TEC anomalies. The aim of this paper is to provide a potential solution of this problem partially. Meanwhile, to exclude other possible activities that induce ionospheric disturbances, we examined the geomagnetic conditions around 8 March 2011. There was a short period of quiet geomagnetic activity from 3 March to 10 March. Therefore, the significant anomalies on 8 March 2011 are unlikely to be resulted from geomagnetic storms, and are most likely related to the 11 March 2011 M9.0 Tohoku earthquake. It is worth noting that there was a M7.2 earthquake occurred on 9 March 2011 approximately 40 km from the 11 March earthquake. The unusual changes of ionospheric TEC might be also the anomalies of the M7.2 earthquake. At present, it is very difficult to separate the anomalies induced by the two large earthquakes due to their short time interval.

The paper only focuses on demonstrating the method for ionospheric data preprocessing to extract the anomaly variations associated with earthquakes. We do not intend to discuss the physical mechanisms of the seismo–ionospheric effects in this paper. The detailed aspects of the possible physical mechanisms were described in many excellent research articles (Park et al., 1993; Molchanov et al., 2004; Namgaladze et al., 2009; Pulinets, 2009; Pulinets and Ouzounov, 2010).

The results in this work showed that the MWT-based method could handle the solar radiation background in the ionospheric TEC, and it requires no prior knowledge about the solar radiation particle composition, no selection of suitable background correction points, and no mathematical assumption of the background distribution. The proposed procedures were illustrated by processing an earthquake that occurred during a period of increasing solar activity, to be an effective and practical tool for background elimination in seismo-ionospheric data analysis. In addition, the MWT-based method can be performed not only for studying ionospheric perturbations of seismic origin but also for other local events, such as typhoons, volcanic eruptions, and anthropogenic effects.

Acknowledgments

This research was supported by the National Important Basic Research Project (973 Program, Grant No. 2011CB707102), the National Natural Science Foundation of China (Grant No. 41104104) and the Key Plan for Introducing Overseas High-level Culture-education Experts. We thank the reviewers for their useful comments and suggestions. The authors acknowledge the International GNSS Service (IGS) and the Center for Orbit Determination in Europe (CODE) for providing the GPS TEC data. The EUV_{26-34} indices were provided by the Space Sciences Center of University of Southern California. The $F_{10.7}$ indices were downloaded from the NGDC database. The geomagnetic indices were obtained from World Data Center C2 for Geomagnetism in Kyoto.

References

Afraimovich, E., Astafyeva, E. TEC anomalies—Local TEC changes prior to earthquakes or TEC response to solar and geomagnetic activity changes? Earth Planets Space 60 (9), 961–966, 2008.

Afraimovich, E., Astafyeva, E., Oinats, A., et al. Global electron content: A new conception to track solar activity. Ann. Geophys. 26 (2), 335–344, 2008.

Bendat, J.S., Piersol, A.G. Random Data: Analysis and Measurement Procedures. Wiley, 2010.

Borovsky, J.E., Thomsen, M.F., Elphic, R.C. The driving of the plasma sheet by the solar wind. J. Geophys. Res. 2 (3), 17617–17639, http://dx.doi.org/10.1029/97JA02986, 1998.

Chen, Y., Chuo, J., Liu, J., et al. A Statistical study of ionospheric precursors of strong earthquakes at Taiwan area. XXVI URSI General Assembly, Toronto, 13–21 Aug. 1999, Abstracts. pp. 745, 1999.

Chen, Y., Liu, J., Tsai, Y., et al. Statistical tests for pre-earthquake ionospheric anomaly. Terr. Atmos. Ocean. Sci. 15 (3), 385–396, 2004.

Daubechies, I. Ten lectures on wavelets. SIAM: Society for Industrial and Applied Mathematics, 377p, 1992. ISBN: 0898712742.

Dautermann, T., Calais, E., Haase, J., et al. Investigation of ionospheric electron content variations before earthquakes in southern California, 2003–2004. J. Geophys. Res. 112, B02106, http://dx.doi.org/10.1029/2006JB004447, 2007.

Dobrovolsky, I., Zubkov, S., Miachkin, V. Estimation of the size of earthquake preparation zones. Pure Appl. Geophys. 117 (5), 1025–1044, 1979.

Grossman, A., Morlet, J. Decomposition of Hardy functions into square integrable wavelets of constant shape. SIAM J. Math. Anal. 15 (4), 723–736, 1984.

Hilton, M.L. Wavelet and wavelet packet compression of electrocardiograms. IEEE T. Bio-Med Eng. 44 (5), 394–402, 1997.

Judge, D.L., McMullin, D.R., Ogawa, H.S., et al. First solar EUV irradiances obtained from SOHO by the CELIAS/SEM. Sol. Phys. 177, 161–173, 1998.

Klimenko, M.V., Klimenko, V.V., Zakharenkova, I.E., et al. Formation mechanism of great positive TEC disturbances prior to Wenchuan earthquake on May 12, 2008. Adv. Space Res. 48 (3), 488–499, 2011.

Kon, S., Nishihashi, M., Hattori, K. Ionospheric anomalies possibly associated with $M \geqslant 6.0$ earthquakes in the Japan area during 1998–2010: Case studies and statistical study. J. Asian Earth Sci. 41 (4), 410–420, 2011.

Le, H., Liu, J., Liu, L. A statistical analysis of ionospheric anomalies before 736 M 6.0+ earthquakes during 2002–2010. J. Geophys. Res. 116, A02303, http://dx.doi.org/10.1029/2010JA015781, 2011.

Liu, J., Chen, Y., Pulinets, S., et al. Seismo-ionospheric signatures prior to $M \geqslant 6.0$ Taiwan earthquakes. Geophys. Res. Lett. 27 (19), 3113–3116, http://dx.doi.org/10.1029/2000GL011395, 2000.

Liu, J., Chen, Y., Jhuang, H., et al. Ionospheric foF2 and TEC anomalous days associated with $M \geqslant 5.0$ earthquakes in Taiwan during 1997–1999. Terr. Atmos. Ocean. Sci. 15 (3), 371–383, 2004a.

Liu, J., Chuo, Y., Shan, S., et al. Pre-earthquake ionospheric anomalies registered by continuous GPS TEC measurements. Ann. Geophys. 22 (5), 1585–1593, 2004b.

Liu, J., Chen, Y., Chuo, Y., et al. A statistical investigation of preearthquake ionospheric anomaly. J. Geophys. Res. 111, A05304, http://dx.doi.org/10.1029/2005JA011333, 2006.

Liu, J., Chen, Y., Chen, C., et al. Seismoionospheric GPS total electron content anomalies observed before the 12 May 2008 Mw7. 9 Wenchuan earthquake. J. Geophys. Res. 114, A04320, http://dx.doi.org/10.1029/2005GL023963, 2009.

Liu, J., Le, H., Chen, Y., et al. Observations and simulations of seismoionospheric GPS total electron content anomalies before the 12 January 2010 M7 Haiti earthquake. J. Geophys. Res. 116, A04302, http://dx.doi.org/10.1029/2010JA015704, 2011.

Mallat, S. Multiresolution approximations and wavelet orthonormal bases of L2 (R). Trans. Amer. Math. Soc. 315 (1), 69–87, 1989a.

Mallat, S. A theory for multiresolution signal decomposition: The wavelet representation. IEEE Tran. Patt. Anal. Mach. Int. 11 (7), 674–693, 1989b.

Mallat, S. A Wavelet Tour of Signal Processing: The Sparse Way, third ed. Academic Press, 2008.

Molchanov, O., Fedorov, E., Schekotov, A., et al. Lithosphere-atmosphere-ionosphere coupling as governing mechanism for preseismic short-term events in atmosphere and ionosphere. Nat. Hazards Earth Syst. Sci. 4 (5/6), 757–767, 2004.

Namgaladze, A., Klimenko, M., Klimenko, V., et al. Physical mechanism and mathematical modeling of earthquake ionospheric precursors registered in total electron content. Geomagn. Aeronomy. 49 (2), 252–262, 2009.

Park, S., Johnson, M., Madden, T., et al. Electromagnetic precursors to earthquakes in the ULF band: A review of observations and mechanisms. Rev. Geophys. 31 (2), 117–132, http://dx.doi.org/10.1029/93RG00820, 1993.

Pulinets, S. Physical mechanism of the vertical electric field generation over active tectonic faults. Adv. Space Res. 44 (6), 767–773, 2009.

Pulinets, S., Boyarchuk, K. Ionospheric Precursors of Earthquakes. Springer Verlag, Berlin, 2004.

Pulinets, S., Ouzounov, D. Lithosphere–atmosphere–ionosphere coupling (LAIC) model – an unified concept for earthquake precursors validation. J. Asian Earth Sci. 41 (4–5), 371–382, 2010.

Rishbeth, H. Ionoquakes: Earthquake precursors in the ionosphere? Eos. Trans. AGU. 87 (32), 316, 2006.

Rishbeth, H. Do earthquake precursors really exist? Eos. Trans. AGU. 88 (29), 296, 2007.

Shao, X., Shao, L., Zhao, G. Extraction of extended X-ray absorption fine structure information from the experimental data using the wavelet transform. Anal. Commun. 35 (4), 135–137, 1998.

Tobiska, W.K. Current status of solar EUV measurements and modeling. Adv. Space Res. 18 (3), 3–10, 1996.

Viereck, R., Puga, L., McMullin, D., et al. The Mg II index: A proxy for solar EUV. Geophys. Res. Lett. 28 (7), 1343–1346, http://dx.doi.org/10.1029/2000GL012551, 2001.

Woods, T.N., Eparvier, F.G., Bailey, S.M., et al. Solar EUV Experiment (SEE): Mission overview and first results. J. Geophys. Res. 110, A01312, http://dx.doi.org/10.1029/2004JA010765, 2005.

Woods, T.N., Eparvier, F.G., Hock, R., et al. Extreme ultraviolet variability experiment (EVE) on the solar dynamics observatory (SDO): Overview of science objectives, instrument design, data products, and model developments. Sol. Phys. 275 (1–2), 115–143, http://dx.doi.org/10.1007/s11207-009-9487-6, 2010.

Xu, T., Chen, Z., Li, C., et al. GPS global electron content and surface latent heat flux variations before the 11 March 2011 M9.0 Sendai earthquake. Adv. Space Res. 48 (5), 1311–1317, 2011.

Zhao, B., Wang, M., Yu, T., et al. Is an unusual large enhancement of ionospheric electron density linked with the 2008 great Wenchuan earthquake? J. Geophys. Res. 113, A11304, http://dx.doi.org/10.1029/2008JA013613, 2008.